HHS Public Access

Author manuscript

Nat Metab. Author manuscript; available in PMC 2019 August 11.

Published in final edited form as:

Nat Metab. 2019 February ; 1(2): 291–303. doi:10.1038/s42255-018-0030-7.

TGF-β2 is an exercise-induced adipokine that regulates glucose and fatty acid metabolism

Hirokazu Takahashi[1,*], **Christiano R. R. Alves**[1,*], **Kristin I. Stanford**[1,2], **Roeland J. W. Middelbeek**[1], **Pasquale Nigro**[1], **Rebecca E. Ryan**[1], **Ruidan Xue**[1,§], **Masaji Sakaguchi**[1], **Matthew D. Lynes**[1], **Kawai So**[1], **Joram D. Mul**[1], **Min-Young Lee**[1], **Estelle Balan**[1], **Hui Pan**[3], **Jonathan M. Dreyfuss**[3], **Michael F. Hirshman**[1], **Mohamad Azhar**[4], **Jarna C. Hannukainen**[5], **Pirjo Nuutila**[5], **Kari K. Kalliokoski**[5], **Søren Nielsen**[6], **Bente K. Pedersen**[6], **C. Ronald Kahn**[1], **Yu-Hua Tseng**[1], and **Laurie J. Goodyear**[1]

[1]Section on Integrative Physiology and Metabolism, Joslin Diabetes Center, Harvard Medical School, Boston, Massachusetts, USA [2]Department of Physiology and Cell Biology, Dorothy M. Davis Heart and Lung Research Institute, The Ohio State University Wexner Medical Center, Columbus, Ohio, USA [3]Bioinformatics Core, Joslin Diabetes Center, Harvard Medical School, Boston, Massachusetts, USA [4]Department of Cell Biology & Anatomy, School of Medicine, University of South Carolina, Columbia, SC, USA [5]Turku PET Centre, University of Turku, Turku, Finland [6]The Centre of Inflammation and Metabolism and the Centre for Physical Activity Research, Rigshospitalet, University of Copenhagen, Denmark

Abstract

Exercise improves health and well-being across diverse organ systems, and elucidating mechanisms underlying the beneficial effects of exercise can lead to new therapies. Here, we show that transforming growth factor-β2 (TGF-β2) is secreted from adipose tissue in response to exercise and improves glucose tolerance in mice. We identify TGF-β2 as an exercise-induced adipokine in a gene expression analysis of human subcutaneous adipose tissue biopsies after exercise training. In mice, exercise training increases TGF-β2 in scWAT, serum, and its secretion

Correspondence should be addressed to Laurie J. Goodyear (laurie.goodyear@joslin.harvard.edu).

§Deceased (December 16, 2016)

*These authors contributed equally to this work

Author contributions

H.T. and C.R.R.A designed research, carried out experiments, analyzed data and wrote the paper. K.I.S. performed experiments with trained mice. R.J.M. performed and analyzed human data. P.N. carried out all experiments of adipocyte incubation. R.E.R carried out experiments and analyzed data with Tgfb2 knockout mice and TGF-β2 treated mice. X.R. designed and performed Seahorse assays and provided human white preadipocytes. M.S. carried out experiments and analyzed data of cell sorting. M.D.L. carried out *in vivo* imaging studies for fatty acid uptake. K.S. and J.D.M. performed genotyping of Tgfb2 knockout mice and cell experiments. J.M.D. carried out correlation analysis of microarray and analyzed bioinformatic data. M.Y.L. carried out gene-expression analysis of human adipose tissue. E.B. carried out fatty acid uptake *in vitro* and Seahorse assays. H.P. and J.M.D. performed bioinformatics analysis. M.F.H. performed *in vivo* experiments and supervised all experiments. M.A. established and provided Tgfb2 knockout mice. J.C.H., K.K.K., B.K.P and S.N. carried out and provided human samples. C.R.K supervised *in vivo* and *in vitro* experiments with adipocytes or adipose tissue. Y.T. supervised experiments with human preadipocytes and provided immortalized brown preadipocytes. L.J.G. directed the research project, designed experiments and wrote the paper. All authors have participated in the manuscript review. All authors approved the final manuscript.

Competing financial interests

The authors have declared that no conflict of interest exists.

from fat explants. Transplanting scWAT from exercise-trained wild type mice, but not from adipose tissue-specific Tgfb2−/− mice, into sedentary mice improves glucose tolerance. TGF-β2 treatment reverses the detrimental metabolic effects of high fat feeding in mice. Lactate, a metabolite released from muscle during exercise, stimulates TGF-β2 expression in human adipocytes. Administration of the lactate-lowering agent dichloroacetate during exercise training in mice decreases circulating TGF-β2 levels and reduces exercise-stimulated improvements in glucose tolerance. Thus, exercise training improves systemic metabolism through inter-organ communication with fat via a lactate-TGF-β2-signaling cycle.

Introduction

Endurance exercise training is an important non-pharmacological strategy to prevent and treat metabolic diseases, including obesity and type 2 diabetes[1–4]. Exercise training can improve whole-body metabolic homeostasis and cause adaptations to multiple tissues throughout the body. In subcutaneous white adipose tissue (scWAT), exercise training decreases cell size and lipid content[5–7], and may reduce inflammation[8–10] and increase the presence of thermogenic brown-like adipocytes or "beige" cells[11–16]. We recently reported that exercise training also has profound effects on the gene expression profile of scWAT in mice, increasing the expression of more than 1500 genes[16]. Transplantation of scWAT from trained mice into sedentary recipient mice improved glucose tolerance and insulin sensitivity, and resulted in metabolic improvements in other tissues, including skeletal muscle and brown adipose tissue (BAT)[16]. These findings led us to hypothesize that exercise-trained scWAT has endocrine effects, inducing adipokines that mediate tissue-to-tissue communication and contribute to the improved metabolic homeostasis with exercise.

TGF-β2 is a member of the *TGF-β* superfamily. *TGF-β2* regulates embryonic development[17–19] and, therefore not surprisingly, global *Tgfb2* null mice exhibit a wide range of developmental defects and perinatal mortality[20]. The phenotype of the *Tgfb2* null mice has no overlap with the *Tgfb1* or *Tgfb3* null mice phenotypes[20–23], indicating that despite the structural similarity, there are different physiological roles among these *TGF-β* isoforms. *TGF-β2* is an immune suppressor involved in the development of immune tolerance[24–26], and recombinant *TGF-β2* incubation is more potent than *TGF-β1* or *TGF-β3* in suppressing macrophage inflammatory responses[26]. In addition, patients with Kawasaki disease, a rare inflammatory disease that affects the small-medium sized arteries, have lower plasma *TGF-β2* concentrations during the acute phase of the disease[27]. The roles of *TGF-β2* in obesity and type 2 diabetes, or in exercise training adaptations, have not been previously described.

Here, we discovere that exercise training increases *TGFB2* mRNA expression in human scWAT. We find that *TGF-β2* is an exercise-induced adipokine that improves glucose tolerance and insulin sensitivity, increases fatty acid uptake and oxidation, and stimulates glucose uptake in skeletal muscle, heart, and BAT. Treatment with recombinant *TGF-β2 in vivo* ameliorates the effects of a high-fat feeding in mice, reduces fat mass and attenuates WAT inflammation. The mechanism by which exercise increases *TGF-β2* in scWAT involves lactate stimulation of gene expression. This study reveals a novel mechanism by which

exercise training regulates whole-body metabolic homeostasis and provides new insight into adipose-muscle tissue cross-talk as a key axis to counteract metabolic diseases.

Results

TGF-β2 is an exercise-induced adipokine

To identify putative adipokines increased by exercise training, we performed microarray analyses in scWAT from healthy young male human subjects[28,29] before and after 12 weeks of moderate intensity endurance cycling exercise training (Supplementary Table 1). In addition, we used our previously published microarray dataset[16] derived from scWAT from mice housed in static cages (sedentary controls) or mice housed in cages with running wheels for 11 days (trained; 6.1 ± 0.4 km of voluntary exercise/day). Genes that were significantly changed by exercise training in humans and mice were further selected by annotation for Extracellular Space in Gene Ontology[30]. Of these genes, the most significantly correlated with the total wheel running distance in the trained mice was *Tgfb2* (Fig. 1a). We validated that exercise training increased *TGFB2* mRNA in scWAT of human subjects using RT-qPCR (Fig. 1b). This led us to hypothesize that *TGF-β2* is an exercise-induced adipokine.

To test this hypothesis we measured *Tgfb2* mRNA levels in different adipose tissue depots after 11 days of voluntary wheel running in mice. Wheel running increased *Tgfb2* mRNA levels by 1.9 ± 0.2 fold in scWAT and by 1.5 ± 0.1 fold in perigonadal white adipose tissue (pgWAT), but there was no effect of exercise training on BAT (Fig. 1c). Exercise training resulted in a pronounced increase in *TGF-β2* protein content in scWAT, but there were no differences in pgWAT, BAT, liver, multiple skeletal muscles, or heart (Fig. 1d-e). Enzyme-linked immunosorbent assays (ELISA) revealed that exercise training of mice for 11 days resulted in significantly higher serum *TGF-β2* concentrations compared to sedentary mice (Fig. 1f). Exercise training in mice fed a high fat diet also increased serum *TGF-β2* concentrations compared to sedentary mice (Fig. 1g). While moderate-intensity cycling exercise training in human subjects[28,29] did not change plasma *TGF-β2* concentrations (Fig. 1h), a training intervention consisting of six weeks of a combination of moderate-intensity continuous training, high-intensity interval training and resistance training increased serum *TGF-β2* concentrations in a cohort of healthy, middle-aged men (Fig 1i). In addition, six sessions of high-intensity cycling exercise training over a period of two weeks[31] tended to increase serum *TGF-β2* concentrations in a group of healthy, middle-aged men (Fig. 1j). Exercise training did not affect *Tgfb1*/*TGFB1* or *Tgfb3*/*TGFB3* in mouse or human WAT (Supplementary Fig. 1a-d).

To determine if changes in *Tgfb2* in scWAT were specific to the exercise stimulus or generalizable to other stimuli known to induce numerous adaptations in WAT[13,32], we measured *Tgfb1–3* in scWAT of mice in response to 5 days of cold exposure, 5 days of β3-agonist treatment, or 14 days of caloric restriction, all treatments which increase beiging of WAT. There was no effect of any of these stimuli on *Tgfb2* mRNA in adipose tissues (Supplementary Fig. 2a-c) and, in fact, beta 3-agonist treatment and caloric restriction decreased the relative expression of *Tgfb1* and *Tgfb3* mRNA in scWAT (Supplementary Fig.

2b,c). These data indicate that increases in *TGF-β2* may be exercise-specific, and not generalizable to all stimuli that regulate scWAT.

Adipose tissue is comprised of mature adipocytes and the stromal vascular fraction (SVF), which consists of several different cell types (preadipocytes, progenitor cells, and immune cells). Our gene expression data were derived from experiments on whole adipose tissue. To determine the cellular component of adipose tissue that secretes *TGF-β2*, we isolated mature adipocytes from the scWAT and pgWAT of sedentary and trained mice and incubated the cells for 3 h in serum-free medium. Concentrations of *TGF-β2* in the media were higher in adipocytes from trained scWAT (Fig. 1k) and pgWAT (Supplementary Fig. 1e) compared to sedentary controls, consistent with the hypothesis that exercise training can induce *TGF-β2* secretion from WAT. Assessment of cells from the stromal vascular compartment of scWAT revealed that exercise training did not alter the relative expression of *Tgfb2* mRNA in endothelial cells or macrophages, but did increase *Tgfb2* mRNA in preadipocytes (Fig. 1l). Together, these data indicate that exercise increases *Tgfb2* specifically in pre- and mature adipocytes.

Our previous work has shown that exercise-induced adaptations to adipose tissue can improve whole-body glucose homeostasis and increase glucose uptake into skeletal muscle and BAT. To determine if *TGF-β2* from WAT mediates some of the effects of exercise training in the body, we used the adiponectin Cre-loxP system to generate adipose-specific *Tgfb2* knockout (*Tgfb2*$^{-/-}$) and flox control (*Tgfb2*$^{f/f}$) mice. *Tgfb2*$^{-/-}$ mice displayed a dramatic decrease in *Tgfb2* mRNA levels in the scWAT, but not in other tissues (Fig. 1m and Supplementary Fig. 3a). Despite lower *Tgfb2* levels in WAT, *Tgfb2*$^{-/-}$ mice had similar circulating levels of *TGF-β2* (Supplementary Fig. 3b), and did not show differences in glucose tolerance, body mass, and running capacity (Supplementary Fig. 3c-f). However, exercise training did not increase circulating levels of *TGF-β2* in *Tgfb2*$^{-/-}$ mice (Fig. 1n). *Tgfb2*$^{-/-}$ mice had normal exercise-induced changes in running capacity, body mass and fat mass (Supplementary Fig. 3g-k), but did not have training-induced improvements in glucose tolerance (Fig 1o).

To investigate the specific contribution of *TGF-β2* from scWAT on glucose tolerance, we transplanted exercise-trained scWAT from *Tgfb2*$^{-/-}$ and *Tgfb2*$^{f/f}$ mice. *Tgfb2*$^{-/-}$ and *Tgfb2*$^{f/f}$ mice were given free access to wheel cages for 11 days (Supplementary Fig. 3l) and the scWAT was transplanted into sedentary recipient mice. Wild-type mice receiving scWAT only from trained *Tgfb2*$^{f/f}$ mice had higher serum TGF-β2 concentrations (Fig. 1p). We have previously shown that mice receiving scWAT from wild type exercise-trained mice have improved glucose tolerance compared to mice transplanted with scWAT from sedentary mice[16]. As expected, mice transplanted with scWAT from trained *Tgfb2*$^{f/f}$ mice had improved glucose tolerance when compared to mice transplanted with scWAT from sedentary *Tgfb2*$^{f/f}$ mice 8 days post-transplantation. However, mice transplanted with scWAT from trained *Tgfb2*$^{-/-}$ mice did not have improved glucose tolerance (Fig. 1q,r). This indicates that scWAT-derived *TGF-β2* contributes to exercise-induced metabolic improvements.

TGF-β2 stimulates glucose and fatty acid uptake *in vitro*

To test whether *TGF-β2* affected metabolism in cell models of multiple tissues, we performed *in vitro* experiments using C2C12 myotubes, 3T3-L1 adipocytes and WT-1 brown adipocytes. Incubation with recombinant *TGF-β2* increased basal, submaximal, and maximal insulin glucose uptake in all 3 cell types (Supplementary Fig. 4a,b). Incubation with recombinant *TGF-β1* or *TGF-β3* had no effect on glucose uptake in C2C12 myotubes (Supplementary Fig. 4c,d). Independent experiments showed that co-incubation of recombinant *TGF-β2* and *TGF-β* receptor inhibitor (LY2109761) blunted the effects of *TGF-β2* in all cell types (Fig. 2a), indicating that this is a receptor mediated response. Consistent with *in vitro* data, T*GF-β2* incubation increased glucose uptake in isolated *soleus* muscle, which was blunted by co-incubation with *TGF-β* receptor inhibitor (Supplementary Fig. 4e). Interestingly, there was no effect of *TGF-β2* on glucose uptake in *extensor digitorum longus* (EDL), a more glycolytic muscle (Supplementary Fig. 4f), suggesting that this effect may be muscle fiber type specific. We also investigated the effects of *TGF-β2* on fatty acid metabolism and found that TGF-β2 incubation increased fatty acid uptake and oxidation in all cell types (Fig 2b). *TGF-β1* incubation did not affect fatty acid uptake and oxidation, but *TGF-β3* incubation also increased fatty acid uptake and oxidation in all cell types (Supplementary Fig. 5a,b). *TGF-β2* incubation, but not *TGF-β1* and *TGF-β3*, stimulated oxygen consumption rate (OCR) in C2C12 myotubes (Fig. 2c), and *TGF-β2* incubation also increased the expression of genes related to mitochondrial biogenesis (Fig. 2d and Supplementary Fig. 5c). We confirmed that *TGF-β2* incubation increased *TGF* signaling as assessed by Smad2 phosphorylation in C2C12 myotubes treated with *TGF-β2* in the absence or presence of a *TGF-β* receptor inhibitor (Supplementary Fig. 6a-d). These data demonstrate that incubation of cells with recombinant *TGF-β2* has significant metabolic effects *in vitro*.

TGF-β2 treatment *in vivo* stimulates tissue glucose uptake

Based on the *in vitro* findings, we next determined if *TGF*-β2 treatment improves glucose tolerance *in vivo*. Normal chow-fed mice infused with *TGF-β2* via osmotic pump increased serum *TGF-β2* concentrations by ~2 fold (Fig. 3a). Nine days of *TGF-β2* infusion improved glucose tolerance (Fig. 3b,c), but did not change insulin tolerance (Fig. 3d). Thirteen days of *TGF-β2* treatment increased contraction- and insulin-stimulated 2-deoxyglucose uptake in *soleus*, basal glucose uptake in heart, and basal and insulin-stimulated glucose uptake in BAT (Fig. 3e). This occurred with no change in glucose uptake in scWAT, pgWAT, or the more glycolytic muscles *gastrocnemius* and *tibialis anterior* (Fig. 3e and Supplementary Fig. 7a). These data indicate that *TGF-β2* treatment improves glucose uptake in mitochondria-enriched oxidative tissues, such as red muscle (*soleus*), BAT, and heart.

Nine days of *TGF-β2* treatment *in vivo* also decreased circulating free fatty acid concentrations in mice (Fig. 3f), but did not change total circulating cholesterol and triglyceride concentrations (Supplementary Fig. 7b,c). To determine whether this might be related to increased fatty acid uptake, we treated mice for nine days with *TGF-β2* and quantified luciferin-conjugated fatty acid uptake. This experiment demonstrated that *TGF-β2* produced a significant increase in fatty acid uptake in the mice (Fig. 3g-i).

Extracellular flux analysis revealed that 13 days of *TGF-β2* infusion stimulated OCR in *soleus*, but not in more glycolytic *flexor digitorum brevis* (FDB) muscle (Fig. 3j and Supplementary Fig. 7d). *TGF-β2* infusion also increased the relative expression of Ppargc1a, Ucp1 and Ucp3 in *soleus*, heart, and BAT (Fig. 3k), which are well characterized as regulators of oxidative metabolism[33–35]. *TGF-β2* infusion did not affect body, lean and fat mass, or food intake in mice (Supplementary Fig. 7e-h). These results show that *TGF-β2* treatment stimulates muscle oxidative metabolism in chow-fed mice independent of changes in food intake and body composition.

TGF-β2 treatment improves metabolism in obese mice

To test the hypothesis that *TGF-β2* would improve glucose homeostasis in an animal model of diet-induced obesity, mice were fed a high fat diet (HFD) for 6 weeks followed by implantation of an osmotic pump containing *TGF-β2* as described above. *TGF-β2* treatment for 9 days resulted in robust improvements in glucose tolerance and insulin sensitivity (Fig. 4a-d). Consistent with these findings, *TGF-β2* treatment for 13 days increased contraction- and insulin-stimulated glucose uptake in *soleus* muscle (Fig. 4e), and insulin-stimulated glucose uptake in *tibialis anterior* and *gastrocnemius* muscles (Supplementary Fig. 8a*).* *TGF-β2* treatment also increased basal and insulin-stimulated glucose uptake in heart, BAT and pgWAT (Fig. 4e), with no effect on glucose uptake in scWAT (Supplementary Fig. 8a). Nine days of *TGF-β2* treatment *in vivo* did not change total circulating cholesterol content (Supplementary Fig. 8b), but decreased circulating triglyceride and free fatty acid concentrations (Fig. 4f and Supplementary Fig. 8c) and increased fatty acid uptake in HFD mice (Fig. 4g-i).

The 13 day *TGF-β2* treatment did not change total body mass (Supplementary Fig. 8d) or muscle, heart, BAT or kidney weights (Fig. 4k). In contrast, total fat and visceral fat as a percentage of body weight, as well as adipose tissue mass, were reduced in the *TGF-β2* treated mice (Fig. 4j,k). Liver mass was also reduced (Fig. 4k), and liver fat content was lower in *TGF-β2* treated HFD mice (Fig. 4l). The effects of *TGF-β2* on body composition were not due to differences in food intake (Supplementary Fig. 8e). Thus, *TGF-β2* treatment improves metabolism and body composition in obese HFD mice.

TGF-β2 treatment reduces high fat diet-induced inflammation

Since obesity is commonly associated with inflammation of pgWAT, we investigated whether *TGF-β2* treatment might also affect inflammatory markers and the number of infiltrated macrophages in pgWAT in HFD mice. As expected, HFD mice had higher levels of pro-inflammatory markers and lower levels of anti-inflammatory markers when compared to normal chow diet-fed mice (Fig 5a,b). *TGF-β2* infusion returned most of these inflammatory markers to control levels (Fig 5a,b). To test the direct effects of *TGF-β2* on macrophages, we isolated primary peritoneal macrophages from chow-fed and HFD mice, and incubated the macrophages with *TGF-β2* for 24h. *TGF-β2* incubation normalized inflammatory markers in HFD mice to the levels of the chow-fed mice (Fig 5c).

We then determined the effect of *TGF-β2* on macrophage infiltration ($F4/80^+$) into the pgWAT. HFD mice had higher infiltrated macrophage content in pgWAT than chow-fed

mice, and *TGF-β2* infusion normalized the infiltrated macrophage content in pgWAT (Fig 5d,e). *TGF-β2* infusion partially normalized infiltrated M1 macrophage ($CD11c^+$ $CD206^-$) content in the scWAT of HFD mice (Fig 5d,f). There was no effect of *TGF-β2* on infiltrated M2 macrophage ($CD11c^-$ $CD206^+$) content (Fig. 5f,g). These findings demonstrate that *TGF-β2* can alter polarization of macrophages and attenuate high fat diet-induced inflammation in adipose tissue. Altogether, these data suggest that *TGF-β2* may treat obesity–induced inflammation and insulin resistance.

Lactate stimulates TGF-β2 expression in adipose tissue

Our data demonstrate that exercise training increases *TGF-β2* in scWAT and that *TGF-β2* has pronounced beneficial effects on glucose and lipid homeostasis. Our next goal was to determine the mechanism by which exercise training increases *TGF-β2* in scWAT. For this purpose we used our sedentary and trained scWAT microarray data[16] to determine the genes and pathways most significantly correlated with *Tgfb2*. Pathway analysis revealed that the organic acid, carboxylic acid, and monocarboxylic acid metabolic processes were highly significant pathways that correlated with *Tgfb2* (Fig. 6a). All of these pathways include the lactate metabolic process, an intriguing finding because increases in circulating lactate are one of the most robust and well characterized responses to exercise. We hypothesized that lactate mediates the exercise-induced increase in *TGF-β2*. Human adipocytes were incubated with different concentrations of lactate followed by measurement of mRNA expression for putative adipokine genes that we selected based on significant correlation with running distance and annotation for extracellular space. Notably, *TGFB2* was one of the genes most affected by lactate, inducing a dose-responsive increase in *TGFB2* mRNA levels (Fig. 6b). Similarly, lactate incubation resulted in a dose dependent increase in *Tgfb2* mRNA levels in 3T3-L1 adipocytes (Fig. 6c). Lactate also increased the concentrations of *TGF-β2* in the media of human and 3T3-L1 adipocytes (Fig. 6d,e). Thus, lactate increases expression of *TGF-β2* in human and mouse adipocytes.

To identify transcription factors regulating this effect, we searched for potential transcriptional factors of *Tgfb2* using the TFBIND tool[36], and assessed which factors had expression that correlated with *TGFB2* in the scWAT microarrays. We found that Arnt, Mecom, and Ppara positively correlated with *TGFB2*. Lactate incubation of human adipocytes did not change *ARNT* and *MECOM* mRNA (Supplementary Fig. 9a,b), but significantly increased *PPARA* mRNA expression (Supplementary Fig. 9c) and PPARα protein content (Supplementary Fig. 9d). Consistent with the hypothesis that PPARα could be a mechanism for exercise-induced lactate regulation of *TGF-β2*, we found that eleven days of voluntary wheel running increased *Ppara* mRNA expression in scWAT of mice (Supplementary Fig. 9e). We also tested the effects of fenofibrate, a potent PPARα agonist, on TGF-β2 concentrations. Fenofibrate incubation of 3T3-L1 adipocytes and scWAT for 24 hours increased *TGF-β2* concentrations in the media (Supplementary Fig. 9f,g), and a single injection of fenofibrate intraperitoneally in mice increased serum TGF-β2 concentrations 24 hours post-injection (Supplementary Fig. 9h).

To determine if lactate exposure *in vivo* increases serum *TGF-β2*, we injected lactate, pyruvate or HEPES (vehicle) intraperitoneally in mice. Only injection of lactate increased

serum lactate concentrations (Supplementary Fig. 10a) and resulted in higher serum *TGF-β2* concentrations (Fig. 6f). Importantly, this lactate effect on serum *TGF-β2* concentrations was fully blunted in Tgfb2$^{-/-}$ mice (Fig. 6g). To investigate the effects of physiological lactate release, we first determined whether wheel running increased serum lactate concentrations over a 24h period and found that mice with access to a wheel cage had higher lactate levels throughout the dark period when compared to sedentary controls (Supplementary Fig. 10b). To determine a causal relationship between lactate and *TGF-β2* secretion, we performed daily injections of the lactate-lowering agent dichloroacetate (DCA) during eleven days of voluntary wheel running in mice. DCA treatment decreased serum *TGF-β2* concentrations in trained mice (Fig. 6h). DCA treatment did not affect running capacity (Supplementary Fig. 10c) or body mass (Supplementary Fig. 10d), but blunted the effects of exercise training on lactate concentrations and glucose tolerance (Fig. 6i and Supplementary Fig. 10d,e). These studies reveal a novel role for lactate in glucose homeostasis by stimulating *TGF-β2* expression and release from scWAT (Fig. 6j).

Discussion

Elucidating mechanisms mediating the profund benefits of exercise on human health has been a major research challenge, with most studies focusing on adaptations to skeletal muscle and the cardiovascular system. In the current study, we establish a novel paradigm in which adipose tissue plays a fundamental role in exercise training adaptations, and we identify a specific, exercise-induced adipokine that regulates exercise effects on metabolism. Our findings indicate that *TGF-β2* is an adipokine that increases with exercise training in humans and mice and functions to promote glucose and fatty acid metabolism. Similar to exercise training, *in vivo TGF-β2* treatment stimulates a host of beneficial metabolic effects, including reversing the detrimental effects of high-fat feeding on glucose tolerance, glucose and fatty acid uptake in skeletal muscle, and modulation of macrophages. These findings demonstrate an important mechanism by which exercise training controls whole-body energy homeostasis; that is, by stimulation of cross-talk between subcutaneous adipose tissue and other metabolic tissues.

While still not fully characterized, it is clear that muscle can release myokines that have been proposed to contribute to the control of whole-body energy metabolism[37,38]. We recently found that transplantation of scWAT from trained mice into sedentary recipient mice improved glucose tolerance and insulin sensitivity, and resulted in metabolic improvements in other tissues, namely skeletal muscle and brown adipose tissue (BAT)[16]. These findings fostered the concept of trained scWAT secreting adipokines that mediate some of the effects of exercise training on metabolism. *TGF-β2* is the first validated exercise-induced adipokine that can stimulate glucose and fatty acid uptake in other tissues, and thus, in addition to the role of skeletal muscle as an exercise-induced secretory organ, scWAT can also function in this manner. Importantly, cold exposure, β3-agonist treatment and caloric restriction, other stimuli that cause several adaptations to scWAT similar to what occurs with exercise, did not affect *Tgfb2* production. This indicates that *TGF-β2* is an exercise-specific adipokine.

Another novel finding of the current study is that lactate stimulates *TGF-β2* expression in human and mouse adipose cells. Voluntary wheel running increased serum concentrations of both lactate and *TGF-β2*, and DCA treatment, a drug that reduces lactate formation by increasing pyruvate oxidation[39], blunted the effects of voluntary wheel running on serum *TGF-β2* concentrations and glucose tolerance in mice. Lactate is the product of anaerobic glycolysis and when skeletal muscle fibers are under energy demand during exercise, there is an increase in the production and release of lactate into the circulation[40]. The fate of lactate produced during exercise has long been established to be the liver, where it is converted to glucose by the Cori cycle. However, lactate may function in other capacities, as incubation of L6 muscle cells with lactate affects transcription factors involved in mitochondrial biogenesis[41] and lactate incubation induces “beiging” in both murine and human white adipose cells[42]. Interestingly, lactate treatment of human adipose cells also increased the expression of other adipokine genes that we observed significantly correlated with the wheel running distance of mice, including GAS6, CYR61, SOD1, IGFBP5, HAPLN1, DAG1, NTF3 and DKK2. Thus, lactate is not only a substrate for the Cori cycle, but also has other functions including serving as a signaling molecule that can regulate white adipose tissue metabolism and its secretome.

The mechanism by which exercise-induced lactate increases *TGF-β2* expression is not known. Adipose tissue expresses metabolite transporters, including the proton-linked monocarboxylate transporters (MCTs) that drive lactate inside the cell to be converted into pyruvate by lactate dehydrogenase. In addition, lactate can activate G-protein coupled receptors (GPRs) in adipocyte membranes[42]. PPARs are important regulators of oxidative metabolism, including mitochondrial biogenesis[43–45]. We found that lactate increased PPARα expression in human adipose cells and 3T3L1 adipocytes. In addition, Ppara mRNA expression correlated positively with *Tgfb2* mRNA expression in the trained scWAT microarray, and exercise training of a separate cohort of mice increased Ppara mRNA. Interestingly, injection of fenofibrate increased serum TGF-β2 concentrations in mice, and mining a previously published scWAT dataset[45], we found that Ppara KO mice had lower *Tgfb2* mRNA expression when compared to wild type control mice. These data raise the possibility that PPARα signaling plays a role in mediating lactate-induced *TGF-β2* production in scWAT, and in future studies it will be important to elucidate the complete signaling pathway from lactate to TGF-β2 production in scWAT.

Treatment with recombinant *TGF-β2* caused remarkable effects in HFD-induced obese mice, including significant improvements in glucose tolerance and insulin sensitivity, reduced percentage of total and visceral fat content, and reductions in circulating triglyceride and free fatty acid concentrations. Obesity is commonly associated with inflammation in adipose tissue[46–48], while exercise training is recognized for inducing anti-inflammatory effects[38,49]. Previous findings showed that voluntary wheel running decreased perigonadal adipose tissue inflammation in mice fed a high fat diet[10,50]. Our current findings demonstrate that *TGF-β2* attenuates adipose tissue inflammation induced by a high fat diet, including normalization of the pro-inflammatory cytokine content in the visceral WAT of HFD mice. Activation of genes involved in inflammation leads to the recruitment of macrophages into the adipose tissue and these infiltrated macrophages release pro-inflammatory cytokines, which can induce insulin resistance via paracrine effects[46]. *TGF-β2*

is an immune suppressor[26,51,52] and previous data demonstrated that recombinant *TGF-β2* incubation suppresses macrophage cytokine production in developing intestine[26]. In our study, *TGF-β2* treatment normalized the content of infiltrated macrophages in scWAT of HFD mice. Thus, we hypothesize that this normalized inflammation may underlie the improved insulin sensitivity and metabolic status observed after *TGF-β2* treatment in HFD mice.

Taken toghether the current findings suggest that *TGF-β2* may offer a new therapeutic opportunity to treat obesity-induced insulin resistance. We found that 13 days of *TGF-β2* treatment in mice did not reveal any tumor or fibrosis in pathological analysis of liver, heart, kidney and brain (data not shown), however, more long-term studies will be needed to determine the safety of *TGF-β2* treatment. In this regard, if *TGF-β2* is to be considered as a therapeutic, it will be important to determine the signaling pathways activated by *TGF-β2* in skeletal muscle tissues in vivo, and carry out more detailed studies on the effects of exercise on *TGF-β2* in human subjects. We clearly show that exercise training increases *TGF-β2* in human scWAT and lactate increases *TGF-β2* in human adipocytes. The effects of exercise training on *TGF-β2* serum concentrations are more variable, and we speculate that this may be due to differences in exercise intensity and duration, time of sampling, and the metabolic state of the subjects. These studies investigating the physiological response of *TGF-β2* to exercise training could provide important information for future therapies.

In conclusion, *TGF-β2* is an exercise-induced adipokine that improves glucose tolerance and insulin sensitivity, and the mechanism by which exercise training increases scWAT *TGF-β2* production involves lactate. This study uncovers a novel mechanism that underlies the effects of endurance exercise training in glucose and lipid metabolism, and opens the perspective to explore the lactate-*TGF-β2* signaling axis to counteract obesity, type 2 diabetes and other metabolic diseases.

Methods

Additional information is available in the Nature Research Reporting Summary linked to this article.

Human experiments

Informed consent was obtained from all human participants and the requirement for written informed consent was waived by the Medical Ethics Committees. Protocols were approved by local Ethical Committee of Copenhagen and Frederiksberg (KF 01 289434) and hospital district of South-Western Finland (28/1801/2013 §228), and were carried out in compliance with the Declaration of Helsinki. *TGFB1*, *2* and *3* mRNA relative expression were analyzed in human scWAT samples. Biopsies of abdominal scWAT and plasma were taken from healthy young male subjects (n = 9–10) before and after 12 weeks of exercise training. The exercise training protocol consisted of 60–80 minutes cycling/day, 5 days/week[28,29]. Serum *TGF-β2* concentration was determined in samples of two additional studies. In the second study (unpublished; NCT03359824), inclusion criteria included age between 18 and 45 years, body mass index of 20 to 25 kg/m^2, normal glucose tolerance, no history of exercise training (exercising < 3 days/week), and VO_{2max} < 40ml/min/kg, measured by submaximal

bicycle ergometer test. Exclusion criteria included chronic diseases, any mental or eating disorder, significant use of alcohol, smoking, use of steroids, narcotics or other substrates, prior exposure to radiation, abnormal cardiovascular status, or physical disability. Training intervention consisted of six weeks of a combination of moderate-intensity continuous training (75–85% of HR_{max}), high-intensity interval training (>90% of HR_{max}) and resistance training. In the third study, samples were obtained from healthy middle-aged sedentary men (n = 10) performed 6 training sessions over a period of 2 weeks[31]. Sessions consisted of 4–6 bouts of cycling for 30 seconds with 4 minutes of recovery between the bouts. Participants were fasted ≥12 hours before blood sampling. Samples were collected before and after the 2-week exercise intervention (72 hours after the last training session).

Cell culture and differentiation

C2C12, 3T3-L1 and WT-1 immortalized cell lines and human immortalized preadipocytes were used in this study. C2C12 and 3T3-L1 lines were purchased from American Type Culture Collection (ATCC). WT-1 cell line and human immortalized preadipocytes were previously generated in the laboratory of Dr. Tseng. C2C12 cells were differentiated to myotubes in Dulbecco's modified eagle medium high glucose (DMEM-H) supplemented with 2% horse serum and 1% Pen/Strep. 3T3-L1 cells were differentiated in DMEM-H supplemented with 10% FBS, 1% Pen/Strep, and MDI (uM isobutylmethylxanthine (IBMX), 167 nM Insulin, 1 uM Dexamethasone) for 2 days after cell confluence (day1–2). Cells were kept in medium containing 100 nM insulin for 2 additional days (day3–4) and maintained in 10% and 1% Pen/Strep without supplement until experiments. WT-1 brown preadipocytes were differentiated in DMEM-H supplemented with 2% FBS, 1% Pen/Strep, 20 nM insulin and 1 nM T3 for 2 days (day1–2) and 0.125 mM indomethacin, 5 uM dexamethasone, and 0.5 mM IBMX were added for an additional 2 days (day 3–4)[53]. Cells were maintained in DMEM-H with 2% FBS, 1% Pen/Strep until experiments. Differentiated C2C12 myotubes, 3T3-L1 adipocytes and WT-1 brown adipocytes were treated with 20ng/ml of recombinant *TGF-β1* (Sigma), *TGF-β2* (Cell Signaling) or *TGF-β3* (R&D Systems) for 24 hours and/or *TGF-β* receptor inhibitor (LY2109761) unless otherwise specified. Differentiated 3T3-L1 adipocytes was also treated with Fenofibrate (ab120832, Abcam). Immortalized human white preadipocytes were previously generated from subcutaneous white adipose tissue[53]. Cells were differentiated[54] and treated with different concentrations of lactate (pH 7.4) for 24h. Primary macrophages were collected from the peritoneal cavity of C57BL/6 mice with injection of 5ml sterile RPMI media (GIBCO). Cells were plated in 24-well dishes. Nonadherent cells were removed by washing after 1 hour to enrich for peritoneal macrophages, which were incubated for 3 hours in DMEM-H supplemented with 10% FBS, 1% Pen/Strep. All cells used in this study were maintained at 37 °C in 5% CO_2. We routinely check for mycoplasma contamination and all the cells used in this study were free of mycoplasma.

Mice and generation of adipose-specific Tgfb2 knockout mice

All animal studies were approved by the Institutional Animal Care and Use Committee (IACUC) of the Joslin Diabetes Center and were in accordance with NIH guidelines. Nine-week-old male C57BL/6 mice (Charles River Laboratories) were used for exercise training studies and nine-week-old male ICR mice (TACONIC) were used for *in vivo TGF-β2*

treatment. Mice were given ad libitum access to standard chow diet (9F 5020 Laboratory Diet, 23% protein, 55% carbohydrate, 22% fat, 3.56 kcal/gm, PharmaServ Inc.) or high fat diet (D12492, 20% protein, 20% carbohydrate, 60% fat, 5.24 kcal/gm, Research Diets, Inc.). For cold exposure and thermoneutral conditions, mice were housed at 5°C or 30°C, respectively, for the indicated times in a controlled environmental chamber (Caron Products & Services Inc., Marietta, OH) with free access to food and water. Body core temperature was determined using a RET-3 rectal probe for mice (Physitemp)[32]. β3-agonist treatment was used to stimulate the browning of white adipose depots. Mice were treated with daily i.p. injections of 1 mg/kg bodyweight CL316,243 (Sigma-Aldrich, St. Louis, MO) dissolved in PBS (also used for control injections) for up to five days[32]. For the caloric restriction experiment, mice had a reduction of 50% in food intake. For running training, mice were singly housed with or without access to a running wheel for 11 or 28 days and voluntary running distance was recorded. The running wheels were locked 12 hours before any test or euthanasia. Mice were housed at 21°C on a 12-h light/dark cycle. Studies aimed at comparing mice housed at 21°C with mice housed in a thermoneutral environment (30°C) were not performed, because mice housed at 30°C ran approximately 42% less than mice housed at 21°C (Supplementary Fig. 11).

We used the adiponectin Cre-loxP system to generate adipose-specific *Tgfb2* knockout (*Tgfb2*$^{-/-}$) and flox control (*Tgfb2*$^{f/f}$) mice. *Tgfb2*^{flox} mice were generated in the Azhar lab[22] and bred with adipoq-Cre mice in-house. Nine to fourteen-week-old male *Tgfb2*$^{f/f}$ and *Tgfb2*$^{-/-}$ mice were used for experimets and littermate controls were used. Tails were genotyped using the following primer sequences, Tgfb2 flox: IMF65 Tgfb2–5’arm CAC CTT TTA CCT ACA GAT GAA GTT GC; IMR65 Tgfb2–3’arm CTT AAG ACC ACA CTG TGA GAT AAT CC; IMR66 LAR3 primer CAA CGG GTT CTT CTG TTA GTC C. Adiponectin cre 18564 Transgene Forward GGA TGT GCC ATG TGA GTC TG; 15381 Transgene Reverse ACG GAC AGA AGC ATT TTC CA; oIMR7338 Internal Positive Control Forward CTA GGC CAC AGA ATT GAA AGA TCT; oIMR7339 Internal Positive Control Reverse GTA GGT GGA AAT TCT AGC ATC ATC C.

TGF-β2 treatment *in vivo* via osmotic pump infusion

Ten-week-old male ICR mice underwent surgery to have Alzet mini-osmotic pumps (DURECT) implanted adjacent to the scWAT fat pad. The osmotic pumps were filled with recombinant *TGF-β2* (8406LC, Cell Signaling Technologies) diluted in phosphate-buffered saline. PBS filled pumps were implanted in the control groups. During 13 consecutive days, mice received 12 ng of *TGF-β2* per Kg of body mass per hour. Glucose tolerance tests (GTTs) or insulin tolerance tests (ITTs) were performed after 9 days of treatment. *In vivo* glucose uptake or tissue collection were performed after 13 days of treatment.

Lactate and fenofibrate injection *in vivo*

Ten-week old male C57BL/6 mice were injected intraperitoneally with 15 uL/g body mass of 300 mM sodium lactate (Sigma) in 5 mmol/L HEPES (pH 7.4), 2g/kg body mass of sodium pyruvate (Sigma) in 5 mmol/L HEPES (pH 7.4) or 5 mmol/L of HEPES (pH 7.4)[55]. Blood was collected from the tail at baseline and 1, 3, 6, 12, and 24 hours after injection and serum was analyzed for *TGF-β2* concentration and lactate concentration. A similar

experiment was performed in Tgfb2$^{f/f}$ and Tgfb2$^{-/-}$ mice and blood was collected from the tail 24 hours after lactate injection. In an additional experiment, C57BL/6 mice were injected intraperitoneally with 100 mg/kg of Fenofibrate (ab120832, Abcam) and blood was collected 24 hours after injection to determine serum *TGF-β2* concentrations.

DCA treatment *in vivo*

Ten-week-old male C57BL/6 mice were individually housed with or without access to a running wheel. Mice received daily intraperitoneal injection with 400 mg/kg of sodium dichloroacetate (DCA; Sigma) in 0.9% saline or 0.9% saline as vehicle. Wheels were locked on day 12 and mice were tested and dissected 48 hours after the last injection of DCA or saline.

Fat transplantation

Fat transplantation was performed using scWAT from sedentary *Tgfb2*$^{f/f}$, trained *Tgfb2*$^{f/f}$ and trained *Tgfb2*$^{-/-}$ donor mice as previously described[16]. Briefly, donor mice were killed by cervical dislocation under isoflurane anesthesia and scWAT was removed and rinsed in phosphate-buffered saline solution in a 37°C water bath. scWAT from each donor mouse was transplanted into the visceral cavity of each recipient mouse under isoflurane anesthesia. Serum GTTs were performed eight days post transplantation to ensure proper recovery from surgery.

In Vivo glucose uptake

Mice were fasted from 7 a.m. to 12 p.m. To measure glucose uptake, mice were anesthetized with pentobarbital sodium (90 mg/kg of body weight) 30 minutes prior to the study. Baseline blood samples were collected from the tail vein prior to intravenous delivery of of a saline or Insulin (16.6 U/kg) and 20% glucose bolus (1.0 g of glucose/kg of body weight), along with [3H]-2-deoxyglucose through the retroorbital sinus. For contraction studies this tracer bolus in saline solution occurred simultaneously with the onset of in situ nerve stimulation. For all treatments, blood samples were taken from the tail vein at 5, 10, 15, 25, 35, and 45 minutes post-injection for the determination of blood glucose and [3H]-2-deoxyglucose specific activity. After collection of the final blood sample, animals were euthanized and tissues were removed and frozen in liquid nitrogen. Accumulation of [3H]-2-deoxyglucose-6-P in tissue was determined via a precipitation protocol using barium hydroxide/zinc sulfate and perchloric acid[56]. In vivo glucose uptake was calculated as a clearance.

In situ muscle contraction

Sciatic nerve from both legs were surgically exposed for electrode placement. While one leg was left unstimulated (basal/sham control), the other leg was subjected to electrical stimulation using a Grass S88 pulse generator for 15 min of contractions (train rate, 1/s; train duration, 500 ms; pulse rate, 100 Hz, duration, 0.1 ms at 2–7 V)[57].

In vitro glucose uptake

In vitro glucose uptake was measured by the accumulation of [^{3}H]-2-deoxyglucose in cells[58]. Cells were serum-starved for 5 h in αMEM prior to any treatment. Cells were

washed twice in PBS and incubated with or without 10 or 100 nM insulin for 30 minutes. Following stimulation, 2-deoxy-D-[^{3}H]glucose uptake was measured by incubating cells at room temperature for 5 min in transport solution (140 mM NaCl, 20 mM Hepes-Na, pH 7.4, 5 mM KCl, 0.5 μCi/ml 2-deoxy-D-[^{3}H]glucose, 2.5 mM MgSO4, 1.0 mM CaCl2). Non-facilitated glucose uptake was determined in the presence of 10 μM cytochalasin B. Net accumulation of ^{3}H-2-deoxyglucose was determined and rates of uptake calculated.

In vitro fatty acid uptake and oxidation

In vitro fatty acid uptake and oxidation were measured using [^{14}C] palmitic acid[59]. Fatty acid oxidation was determined by measuring the conversion of ^{14}C-labeled palmitic acid into CO_2. Briefly, cells were incubated with HEPES buffered saline containing 5 mM glucose and DMEM containing 4% FFA-free albumin, 0.5 mM Palmitic acid and 0.2 μCi/ml [1-^{14}C]-palmitic acid for fatty acid oxidation assay. After one hour, HEPES buffered saline or DMEM was transferred to a vial containing Acetic acid (1M), capped quickly and incubated for 1 hr for CO_2 gas to be released. Released $^{14}CO_2$ was absorbed by hyamine hydroxide in a center well and activity was counted. Fatty acid uptake was determined by washing the cells incubated in [1-^{14}C]-palmitic acid with PBS and lipids were extracted from cells using a chloroform-methanol mixture (2:1), and ^{14}C counts in the organic phase were counted. Protein concentrations were determined using the by Bradford assay (Bio-Rad) and fatty acid uptake and oxidation were normalized to protein content.

In vivo bioluminescent fatty acid uptake

For *in vivo* fatty acid uptake experiments, FVB-Tg(CAG-luc,-GFP)L2G85Chco/J mice (Jackson Laboratory) were treated with *TGF-β2* or vehicle via osmotic infusion pump as described above. After 13 days, mice were injected retro-orbitally with 2um of a fatty acid-luciferin conjugate (FFA-SS-Luc Intrace Medical SA; Lausanne, Switzerland) and imaged using IVIS Spectrum CT. In this study, mice were anesthetized with isofluorane and imaged using sequential 30 s exposures for 12 minutes and area under the curve was calculated and compared between experimental groups. Data was analyzed using Living Image Software.

Extracellular flux analysis (Seahorse)

Mitochondrial oxidative phosphorylation in differentiated C2C12 cells treated with recombinant *TGF-β1*, *TGF-β2* and *TGF-β3* proteins were analyzed using extracellular flux analysis (XF24, Agilent Seahorse, MA USA) in sodium bicarbonate-free DMEM supplemented with 31.7 mM NaCl, 10 mM glucose and 2mM glutamax (pH 7.4 adjusted using NaOH). Oxygen consumption rates (OCR) were measured at baseline and traced in real-time after sequential injections of oligomycin (0.5 uM final concentration), carbonyl cyanide-4-(trifluoromethoxy) phenylhydrazone (FCCP; 0.33 uM final concentration), and rotenone (0.5 uM final concentration) as previously described[60].

For ex vivo experiments, extracellular flux analysis was measured with muscle fibers isolated from *soleus* and *flexor digitorum brevis* (FDB) from mice treated with *TGF-β2* according to the modified manufacturer's protocol. Muscles were dissected, rinsed with phosphate-buffered saline and incubated for 90 minutes in dissociation medium (pH 7.2) composed of DMEM high glucose (#11965092, Gibco, Thermo Fisher Scientific Inc., MA,

USA), gentamycin (#G1397, Sigma-Aldrich, USA), 2% FBS, and 4 mg/ml collagenase A (#11088785103, Sigma-Aldrich, USA) and then single myofibers were isolated. Growth Factor Reduced Matrigel Matrix (BD) was diluted 1:1 in DMEM and used to coat (3uL) each well of Seahorse XF24 Cell Culture Microplates. Myofibers were plated and incubated in assay buffer (120 mM NaCl, 3.5 mM KCl, 1.3 mM CaCl2, 0.4 mM KH2PO4, 1 mM MgCl2, 5 mM HEPES and 15 mM D-glucose adjusted to pH 7.4) at 37 °C in 5% CO_2 environment for 30 minutes and a CO2 free incubator at 37°C for 1 hour before analysis. Oxygen consumption rates (OCR) were measured at baseline and traced in real-time after sequential injections of oligomycin (0.8 ug/ml final concentration), FCCP (400 nM final concentration), and antimycin (1uM final concentration for myofibers from FDB and 3 uM for those from *soleus*).

Cell sorting

Stromal vascular fraction (SVF) was obtained from pgWAT by treatment with 2 mg/mL collagenase (Sigma) for 45 min at 37 °C. The isolated SVF was resuspended in cold Hank's balanced salt solution (HBSS) with 2% fetal bovine serum (FBS). Cells were incubated with CD45-PE-Cy7 (eBiosciences), F4/80-APC-Cy7 (BioLegend), CD206-Alex647 (Serotec, Inc.) and CD11c-PE (BD Pharmingen) antibodies for 30 min in HBSS containing 2% FBS on ice and then washed and resuspended in solution with Sytox Blue (Thermo Scientific). Cells were analyzed on a BD FACSAria cell sorter after selection by forward scatter and side scatter, followed by exclusion of dead cells with Sytox Blue staining, and analyzed for cell-surface markers using FlowJo software (Tree Star). M1 or M2 macrophages were identified as F4/80-positive/CD11c-positive/CD206-negative or F4/80-positive/CD11c-negative/CD206-positive cells, respectively. The data are shown as the percentage of M1 and M2 macrophages. For sorting preadipocytes, endothelial cells and macrophages, cells were incubated with CD31-PE-Cy7 (eBiosciences), F4/80-APC (eBiosciences), and Sca-1 FITC (eBiosciences) antibodies for 30 min in HBSS containing 2% FBS on ice and then washed and resuspended in solution with Propidium Iodide Staining Solution (Sigma). Gating strategies are presented in Supplementary Figure 12 and Supplementary Figure 13.

Enzyme-Linked Immunosorbent Assay (ELISA) and serum lactate levels

Serum and media total *TGF-β2* levels were determined using an enzyme-linked immunosorbent assay (ELISA), according to the manufacturer's protocol (MBS703270, MyBioSource, San Diego, CA for mouse serum and media, and DB250, R&D Systems for human serum). Triglyceride, cholesterol and free fatty acid levels were determined using commercially available ELISA kits (Crystal Chem Inc. or Alpco Diagnostics, USA). Serum lactate was determined using spectrophotometric technique[61].

Quantitative RT-qPCR

RNA was isolated from tissue using a RNA extraction kit (Direct-zol™ RNA MiniPrep, Zymo Research, Irvine, CA). RNA was reverse-transcribed using standard reagents (High Capacity Reverse Transcription Kits, Applied Biosystems) and cDNA was amplified with Power SYBR Green PCR master mix (Applied Biosystems), using the ABI 7900HT real-time PCR system. For each gene, mRNA expression was calculated relative to Gapdh. Genes that were never detected were excluded from Fig 6b. Primer sequences used in RT-qPCR for

mice and human samples are presented in Supplementary Table 2 and Supplementary Table 3, respectively.

Western blotting

Tissue samples were homogenized in lysis buffer (50 mM Tris HCl, 1 mM EDTA, 1 mM EGTA, 10% Glycerol, 1% Triton-X, 50 mM NaF, 5 mM Na Pyrophosphate, Protease Inhibitor Cocktail, DTT) and protein concentrations were determined by Bradford assay (Bio-Rad). Protein samples were run on a 15% SDS-PAGE gel, transferred to a nitrocellulose membrane, and blocked in 5% milk. Primary antibodies were incubated overnight and used to probe for *TGF-β2* (SC-90, Santa Cruz Biotechnology, Santa Cruz, CA), PPARα (SC-9000, Santa Cruz Biotechnology, Santa Cruz, CA), SMAD2 (5339, Cell Signaling Technology, Beverly, MA), pSMAD2 (3101, Cell Signaling Technology, Beverly, MA), and GAPDH (2118S, Cell Signaling Technology, Beverly, MA). Membranes were imaged using the ChemiDoc Touch System (Bio-Rad). Original uncropped western blot images are presented in the Supplementary Information.

Bioinformatic analysis

We normalized our previously published mouse microarray dataset[16] with the dChip software[62]. We tested between group differential expression using the R package limma[63]. To test correlation of probesets to the *TGF-β2* probeset (1423250_a_at), we first removed each probeset's average training effect, so that probesets affected by exercise training would not correlate by default. Then we tested correlation for each probeset to *TGF-β2* using the R function cor.test. We similarly tested GO Biological Process pathways from the Molecular Signature Database[64] by removing the training effect then testing correlation with *TGF-β2* using the NEk* statistic from the R package sigPathway[65]. To identify potential transcription factors that regulate TGF-β2, we downloaded the 3604bp TGF-β2 promoter sequence (Mus musculus strain C57BL/6J chromosome 1, 186711212–186707709) from the NCBI gene database, and searched for transcription factor binding sites in the TFBIND database (http://tfbind.hgc.jp/). We tested for positive correlation of these transcription factors to Tgfbp2 using a one-sided test in the trained mice by looking at the most correlated probeset per gene. For the heatmap, $\log_2$ gene expression data were centered to have a mean of zero and restricted to the interval [−2,2], along with a color bar representing lactate concentration at the top.

We normalized the human microarray data using Robust Multi-array Average (RMA). We analyzed within subject differences before vs. after exercise using a paired analysis with limma[63]. Bioinformatic analyses were done in the R/Bioconductor software[66].

Statistical analysis

Data are expressed as mean ± s.e.m or box plots (min to max) with dots as individual values. Sample size are indicated in the figure legends. Statistical analyses were performed using GraphPad Prism 7 software (GraphPad Software, Inc.). Unpaired (or paired for human data) two-tailed Student's t-test was used to compare two experimental groups. One-way or repeated measurement analysis of variance (ANOVA), followed by Tukey's multiple comparisons test, were applied to compare three or more groups or to compare groups

within different time points. Pearson correlation coefficient was used to measure linear correlation between two variables. No statistical method was used to predetermine sample size. All experiments were not blinded. In all cases, we assumed equal variance. Statistical significance was defined as $P < 0.05$.

Data availability

All data underlying the findings reported in this manuscript are provided as part of the article. Source data are available online. Mouse and human microarray data are available at the Gene Expression Omnibus (GEO) GSE68161 and GSE116801. The raw data that are not already presented in the figures are available from the corresponding author upon reasonable request. Correspondence and requests for materials should be addressed to L.J.G.

Supplementary Material

Refer to Web version on PubMed Central for supplementary material.

Acknowledgements

This work was supported by NIH grants R01DK099511 and R01DK101043 (to L.J.G.), K23DK114550 (to R.J.W.M), and the Joslin Diabetes Center DRC (P30 DK36836). H.T. was supported by individual research fellowships from the Uehara Memorial Foundation and Sumitomo Life Welfare Foundation. Y.H.T. was supported by NIH grant grants R01DK077097 and R01DK102898. K.I.S was supported by R01-HL138738. M.D.L. was supported by NIH grants T32DK007260, F32DK102320, and K01DK111714. M.A. was supported by NIH grant R01HL126705 and American Heart Association Grant-in-Aid grant 17GRNT33650018. B.K.P. and the Centre for Physical Activity Research is supported by a grant from TrygFonden. We thank Kallie Longval and Allen Clermont from the Joslin Diabetes Center Animal Physiology Core, and Lakshmilatha Kannan from Joslin Special Assay Core. We thank Drs. Leslie Rowland, Sarah Lessard and Andre Queiroz for helpful scientific discussions, and Noah Prince and Christian Doherty for technical support.

References

1. Stanford KI & Goodyear LJ Exercise and type 2 diabetes: molecular mechanisms regulating glucose uptake in skeletal muscle. Adv. Physiol. Educ 38, 308–314 (2014). [PubMed: 25434013]
2. Fiuza-Luces C, Garatachea N, Berger NA & Lucia A Exercise is the Real Polypill. Physiology 28, 330–358 (2013). [PubMed: 23997192]
3. Booth FW, Roberts CK & Laye MJ Lack of exercise is a major cause of chronic diseases. Compr. Physiol. (2012). doi:10.1002/cphy.c110025.Lack
4. Colberg SR et al. Exercise and type 2 diabetes: The American College of Sports Medicine and the American Diabetes Association: Joint position statement. Diabetes Care 33, (2010).
5. Gollisch KSC et al. Effects of exercise training on subcutaneous and visceral adipose tissue in normal- and high-fat diet-fed rats. Am. J. Physiol. Endocrinol. Metab 297, 495–504 (2009).
6. Stanford KI & Goodyear LJ Muscle-Adipose Tissue Cross Talk. Cold Spring Harb. Perspect. Med 4, a029801 (2017).
7. Craig BW, Hammons GT, Garthwaite SM, Jarett L & Holloszy JO Adaptation of fat cells to exercise: response of glucose uptake and oxidation to insulin. Journal of applied physiology: respiratory, environmental and exercise physiology 51, 1500–6 (1981).
8. You T, Arsenis NC, Disanzo BL & Lamonte MJ Effects of exercise training on chronic inflammation in obesity: current evidence and potential mechanisms. Sports Med. 43, 243–56 (2013). [PubMed: 23494259]
9. Porter JW et al. Anti-inflammatory effects of exercise training in adipose tissue do not require FGF21. J. Endocrinol 235, 97–109 (2017). [PubMed: 28765264]
10. Kawanishi N, Yano H, Yokogawa Y & Suzuki K Exercise training inhibits inflammation in adipose tissue via both suppression of macrophage infiltration and acceleration of phenotypic switching

from M1 to M2 macrophages in high-fat-diet-induced obese mice. Exerc. Immunol. Rev 16, 105–118 (2010). [PubMed: 20839495]

11. Rao RR et al. Meteorin-like is a hormone that regulates immune-adipose interactions to increase beige fat thermogenesis. Cell 157, 1279–1291 (2014). [PubMed: 24906147]
12. Bostrom P et al. A PGC1 alpha dependent myokine that drives brown fat like development of white fat and thermogenesis. Nature 481, 463–8 (2012). [PubMed: 22237023]
13. Kajimura S, Spiegelman BM & Seale P Brown and beige fat: Physiological roles beyond heat generation. Cell Metabolism 22, 546–559 (2015). [PubMed: 26445512]
14. Stallknecht B, Vinten J, Ploug T & Galbo H Increased activities of mitochondrial enzymes in white adipose tissue in trained rats. Am. J. Physiol 261, E410–E414 (1991). [PubMed: 1653528]
15. Trevellin E et al. Exercise training induces mitochondrial biogenesis and glucose uptake in subcutaneous adipose tissue through eNOS-dependent mechanisms. Diabetes 63, 2800–2811 (2014). [PubMed: 24622799]
16. Stanford KI et al. A Novel Role for Subcutaneous Adipose Tissue in Exercise-Induced Improvements in Glucose Homeostasis. Diabetes 64, 2002–2014 (2015). [PubMed: 25605808]
17. Massague J TGF-b signal transduction. Annu Rev Biochem 67, 753–791 (1998). [PubMed: 9759503]
18. LEASK A TGF- signaling and the fibrotic response. FASEB J. 18, 816–827 (2004). [PubMed: 15117886]
19. Li MO, Wan YY & Flavell RA T Cell-Produced Transforming Growth Factor-β1 Controls T Cell Tolerance and Regulates Th1- and Th17-Cell Differentiation. Immunity 26, 579–591 (2007). [PubMed: 17481928]
20. Sanford LP et al. TGFbeta2 knockout mice have multiple developmental defects that are non-overlapping with other TGFbeta knockout phenotypes. Development 124, 2659–2670 (1997). [PubMed: 9217007]
21. Doetschman T et al. Generation of mice with a conditional allele for the transforming growth factor beta3 gene. Genesis 50, 59–66 (2012). [PubMed: 22223248]
22. Ishtiaq Ahmed AS, Bose GC, Huang L & Azhar M Generation of mice carrying a knockout-first and conditional-ready allele of transforming growth factor beta2 gene. Genesis 52, 817–826 (2014). [PubMed: 24895296]
23. Azhar M, Yin M, Bommireddy R, Duffy JJ, Yang J, Pawlowski SA, Boivin GP, Engle SJ, Sanford LP, Grisham C, Singh RR, Babcock GF, D. T. Generation of Mice With a Conditional Allele for Transforming Growth Factor beta 1 Gene. Genesis 47, 423–31 (2009). [PubMed: 19415629]
24. de Martin R et al. Complementary DNA for human glioblastoma-derived T cell suppressor factor, a novel member of the transforming growth factor-beta gene family. EMBO J. 6, 3673–7 (1987). [PubMed: 3322813]
25. Zhang H, Yang P, Zhou H, Meng Q & Huang X Involvement of Foxp3-expressing CD4+ CD25+ regulatory T cells in the development of tolerance induced by transforming growth factor-beta2-treated antigen-presenting cells. Immunology 124, 304–14 (2008). [PubMed: 18266851]
26. Maheshwari A et al. TGF-??2 suppresses macrophage cytokine production and mucosal inflammatory responses in the developing intestine. Gastroenterology 140, 242–253 (2011). [PubMed: 20875417]
27. Shimizu C et al. Transforming growth factor-beta signaling pathway in patients with Kawasaki disease. Circ. Cardiovasc. Genet 4, 16–25 (2011). [PubMed: 21127203]
28. Yfanti C et al. Effect of antioxidant supplementation on insulin sensitivity in response to endurance exercise training. Am. J. Physiol. Endocrinol. Metab 300, E761–70 (2011). [PubMed: 21325105]
29. Yfanti C et al. Antioxidant Supplementation Does Not Alter Endurance Training Adaptation. Med. Sci. Sports Exerc 42, 1388–1395 (2010). [PubMed: 20019626]
30. Camon E The Gene Ontology Annotation (GOA) Database: sharing knowledge in Uniprot with Gene Ontology. Nucleic Acids Res 32, 262D–266 (2004).
31. Motiani P et al. Decreased insulin-stimulated brown adipose tissue glucose uptake after short-term exercise training in healthy middle aged men. Diabetes, Obes. Metab (2017). doi:10.1111/dom.12947

32. Schulz TJ et al. Brown-fat paucity due to impaired BMP signalling induces compensatory browning of white fat. Nature 495, 379–383 (2013). [PubMed: 23485971]
33. Rasbach K. a. et al. PGC-1α regulates a HIF2α-dependent switch in skeletal muscle fiber types. PNAS 107, 21866–21871 (2010). [PubMed: 21106753]
34. Wu Z et al. Mechanisms controlling mitochondrial biogenesis and respiration through the thermogenic coactivator PGC-1. Cell 98, 115–124 (1999). [PubMed: 10412986]
35. Cohen P et al. Ablation of PRDM16 and beige adipose causes metabolic dysfunction and a subcutaneous to visceral fat switch. Cell 156, 304–316 (2014). [PubMed: 24439384]
36. Tsunoda T & Takagi T Estimating transcription factor bindability on DNA. Bioinformatics 15, 622–630 (1999). [PubMed: 10487870]
37. Stanford KI & Goodyear LJ Muscle-Adipose Tissue Cross Talk. Cold Spring Harb. Perspect. Med 4, a029801 (2017).
38. Benatti FB & Pedersen BK Exercise as an anti-inflammatory therapy for rheumatic diseases—myokine regulation. Nat. Rev. Rheumatol 11, 86–97 (2014). [PubMed: 25422002]
39. Stacpoole PW, Nagaraja NV & Hutson AD Efficacy of dichloroacetate as a lactate-lowering drug. J. Clin. Pharmacol 43, 683–691 (2003). [PubMed: 12856382]
40. Goodwin ML, Harris JE, Hernández A & Gladden LB Blood lactate measurements and analysis during exercise: a guide for clinicians. J. Diabetes Sci. Technol 1, 558–69 (2007). [PubMed: 19885119]
41. Hashimoto T, Hussien R, Oommen S, Gohil K & Brooks G a. Lactate sensitive transcription factor network in L6 cells: activation of MCT1 and mitochondrial biogenesis. FASEB J. 21, 2602–2612 (2007). [PubMed: 17395833]
42. Carrière A et al. Browning of white adipose cells by intermediate metabolites: An adaptive mechanism to alleviate redox pressure. Diabetes 63, 3253–3265 (2014). [PubMed: 24789919]
43. Gulick T, Cresci S, Caira T, Moore DD & Kelly DP The peroxisome proliferator-activated receptor regulates mitochondrial fatty acid oxidative enzyme gene expression. Proc. Natl. Acad. Sci. U. S. A 91, 11012–6 (1994). [PubMed: 7971999]
44. Ahmadian M et al. PPARγ signaling and metabolism: the good, the bad and the future. Nat. Med 99, 557–566 (2013).
45. Li P, Zhu Z, Lu Y & Granneman JG Metabolic and cellular plasticity in white adipose tissue II: role of peroxisome proliferator-activated receptor-alpha. Am. J. Physiol. Endocrinol. Metab 289, E617–E626 (2005). [PubMed: 15941786]
46. Schenk S, Saberi M & Olefsky JM Insulin sensitivity: Modulation by nutrients and inflammation. Journal of Clinical Investigation 118, 2992–3002 (2008). [PubMed: 18769626]
47. Greenberg AS & Obin MS Obesity and the role of adipose tissue in inflammation and metabolism. Am. J. Clin. Nutr 83, 461–465 (2006).
48. Xu H et al. Chronic inflammation in fat plays a crucial role in the development of obesity-related insulin resistance. J. Clin. Invest 112, 1821–30 (2003). [PubMed: 14679177]
49. Gleeson M et al. The anti-inflammatory effects of exercise: Mechanisms and implications for the prevention and treatment of disease. Nature Reviews Immunology (2011). doi:10.1038/nri3041
50. Bradley RL, Jeon JY, Liu F & Maratos-flier E Voluntary exercise improves insulin sensitivity and adipose tissue inflammation in diet-induced obese mice. Am J Physiol Endocrinol Metab (2008). doi:10.1152/ajpendo.00309.2007.
51. de Martin R et al. Complementary DNA for human glioblastoma-derived T cell suppressor factor, a novel member of the transforming growth factor-beta gene family. EMBO J. 6, 3673–7 (1987). [PubMed: 3322813]
52. Zhang H, Yang P, Zhou H, Meng Q & Huang X Involvement of Foxp3-expressing CD4+ CD25+ regulatory T cells in the development of tolerance induced by transforming growth factor-beta2-treated antigen-presenting cells. Immunology 124, 304–14 (2008). [PubMed: 18266851]
53. Xue R et al. Clonal analyses and gene profiling identify genetic biomarkers of the thermogenic potential of human brown and white preadipocytes. Nat. Med 21, 760–768 (2015). [PubMed: 26076036]

54. Shamsi F & Tseng YH in Methods in Molecular Biology 1566, 77–85 (2017). [PubMed: 28244042]
55. Hoque R, Farooq A, Ghani A, Gorelick F & Mehal WZ Lactate reduces liver and pancreatic injury in toll-like receptor- and inflammasome-mediated inflammation via gpr81-mediated suppression of innate immunity. Gastroenterology 146, 1763–1774 (2014). [PubMed: 24657625]
56. Ferré P, Leturque a, Burnol a F., Penicaud L & Girard J A method to quantify glucose utilization in vivo in skeletal muscle and white adipose tissue of the anaesthetized rat. Biochem. J (1985). doi: 10.1042/bj2280103
57. Kramer HF et al. AS160 regulates insulin- and contraction-stimulated glucose uptake in mouse skeletal muscle. J. Biol. Chem. (2006). doi:10.1074/jbc.M605461200
58. Ho RC, Alcazar O, Fujii N, Hirshman MF & Goodyear LJ p38gamma MAPK regulation of glucose transporter expression and glucose uptake in L6 myotubes and mouse skeletal muscle. Am. J. Physiol. Regul. Integr. Comp. Physiol 286, R342–9 (2004). [PubMed: 14592936]
59. Lynes MD et al. The cold-induced lipokine 12,13-diHOME promotes fatty acid transport into brown adipose tissue. Nat. Med 23, 631–637 (2017). [PubMed: 28346411]
60. Townsend KL et al. Increased Mitochondrial Activity in BMP7-Treated Brown Adipocytes, Due to Increased CPT1- and CD36-Mediated Fatty Acid Uptake. Antioxid. Redox Signal 19, 243–257 (2013). [PubMed: 22938691]
61. De Keijzer MH, Brandts RW & Brans PGW Evaluation of a biosensor for the measurement of lactate in whole blood. Clin. Biochem 32, 109–112 (1999). [PubMed: 10211626]
62. Li C Automating dChip: Toward reproducible sharing of microarray data analysis. BMC Bioinformatics 9, (2008).
63. Ritchie ME et al. Limma powers differential expression analyses for RNA-sequencing and microarray studies. Nucleic Acids Res 43, e47 (2015). [PubMed: 25605792]
64. Subramanian A et al. Gene set enrichment analysis: A knowledge-based approach for interpreting genome-wide expression profiles. Proc. Natl. Acad. Sci 102, 15545–15550 (2005). [PubMed: 16199517]
65. Tian L et al. Discovering statistically significant pathways in expression profiling studies. Proc. Natl. Acad. Sci 102, 13544–13549 (2005). [PubMed: 16174746]
66. Gentleman R et al. Bioconductor: open software development for computational biology and bioinformatics. Genome Biol 5, R80 (2004). [PubMed: 15461798]

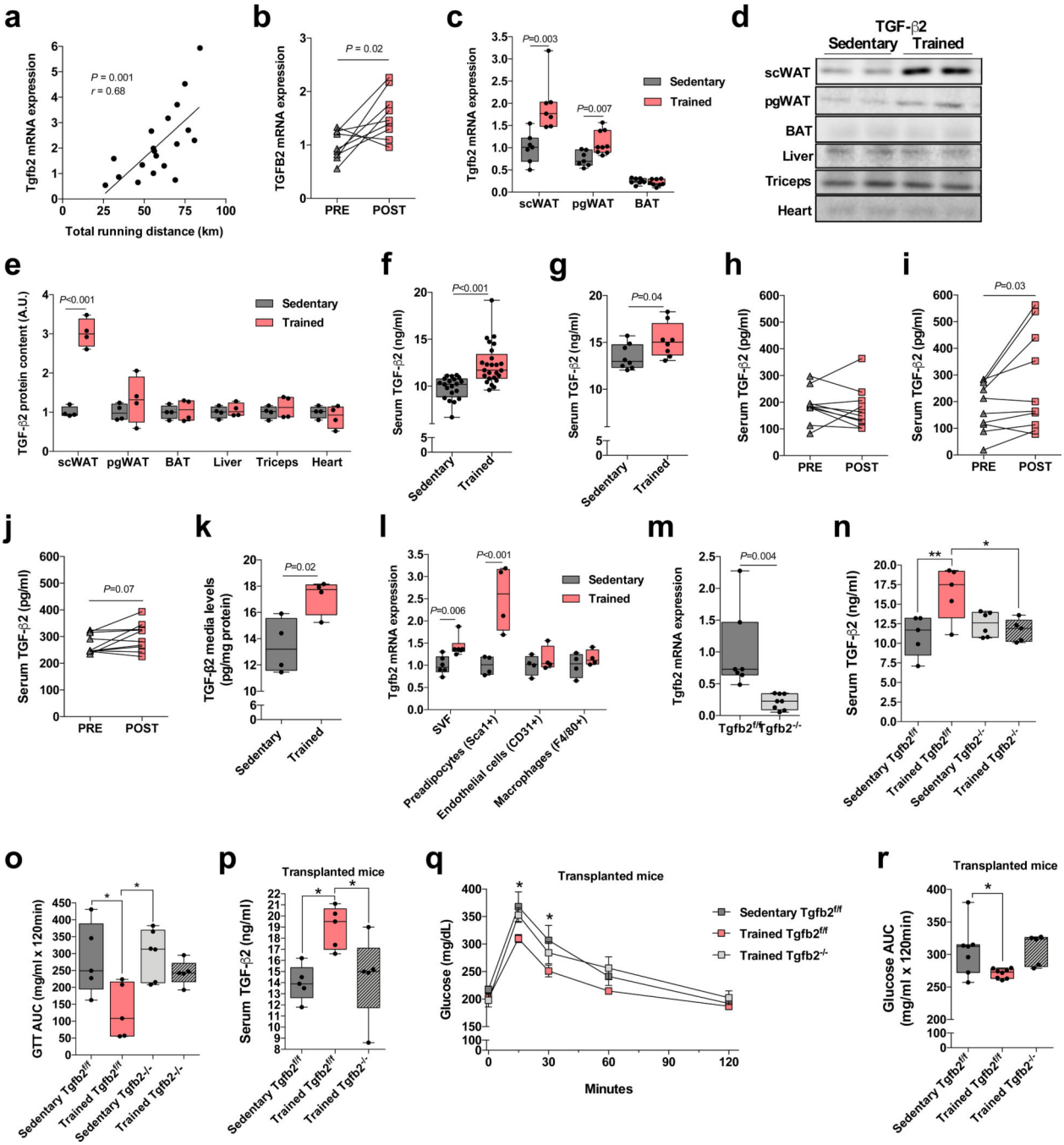

Figure 1.

TGF-β2 is an exercise-induced adipokine. (**a**) Pearson correlation coefficient was used to determine the correlation between Tgfb2 mRNA expression and running distance in trained mice; *n*=19 mice. (**b**) Tgfb2 mRNA expression in human scWAT pre-and post-aerobic exercise training; *n*=9 subjects. (**c**) Tgfb2 mRNA expression in scWAT, pgWAT and BAT in sedentary and trained mice; *n*=7 (scWAT), 8 (pgWAT) and 7 (BAT) sedentary mice, and *n*=7 (scWAT), 9 (pgWAT) and 8 (BAT) trained mice. (**d**) Representative immunoblot and (**e**) quantification of TGF-β2 content in adipose tissue, liver, triceps, and heart of sedentary and

trained mice. *n*=4 mice. (**f**) Serum TGF-β2 concentrations; *n*=20 sedentary mice, *n*=25 trained mice. (**g**) Serum TGF-β2 concentrations in sedentary and trained mice fed a high fat diet; *n*=8 mice. (**h**) Serum TGF-β2 concentrations in healthy subjects pre-and post-12 weeks of moderate-intensity exercise training; *n*=9 subjects. (**i**) Serum TGF-β2 concentrations in healthy subjects pre-and post-6 weeks of a combined aerobic and resistance exercise training protocol; *n*=10 subjects. (**j**) Serum TGF-β2 concentrations in healthy subjects pre-and post-two weeks of high-intensity cycling exercise trainin; *n*=10 subjects. (**k**) TGF-β2 concentrations were determined in the media of mature adipocytes isolated from sedentary and trained scWAT. Each datapoint represents pooled fat pads from 3 mice. *n*=4 biologically independent samples. (**l**) Tgfb2 mRNA expression in stromal vascular fraction, preadipocytes, endothelial cells, and macrophages isolated from scWAT; *n*=4 mice. (**m**) Tgfb2 mRNA expression in scWAT of adipose-specific Tgfb2 knockout ($Tgfb2^{-/-}$) and control ($Tgfb2^{f/f}$) mice; *n*=7 $Tgfb2^{f/f}$ and 8 $Tgfb2^{-/-}$ mice. (**n**) Serum TGF-β2 concentrations in sedentary and trained $Tgfb2^{f/f}$ and $Tgfb2^{-/-}$ mice; *n*=5 or 6 mice/group. (**o**) Glucose tolerance test (GTT) area under the curve in trained $Tgfb2^{f/f}$ and $Tgfb2^{-/-}$ mice. *n*=5 or 6 mice/group. (**p**) Serum TGF-β2 concentrations in recipient mice transplanted with scWAT from trained $Tgfb2^{-/-}$ mice. *n*=5 mice/group. (**q**) GTT and (**r**) GTT area under the curve in recipient mice transplanted with scWAT from trained $Tgfb2^{-/-}$ mice. *n*=7 Sedentary $Tgfb2^{f/f}$, *n*=8 Trained $Tgfb2^{f/f}$, *n*=5 Trained $Tgfb2^{-/-}$. Data are presented as box plots (min, max, median, and 25th and 75th percentiles) with dots as individual values (**c**, **e**, **f**, **g**, **k**, **l**, **m**, **n**, **o**, **p**, **r**), mean ± s.e.m (**q)** or individual values (**a**, **b**, **h**, **i**, and **j**). Paired two-tailed Student's t-tests were used for **b, h, I** and **j**. Unpaired two-tailed Student's t-tests were used for **c, e, f, g, k, l** and **m**. ANOVA was used for **n**, **o**, **p**, **q** and **r**. When ANOVA showed $P<0.05$, Tukey's multiple comparisons tests were used with $*P<0.05$; $**P<0.01$.

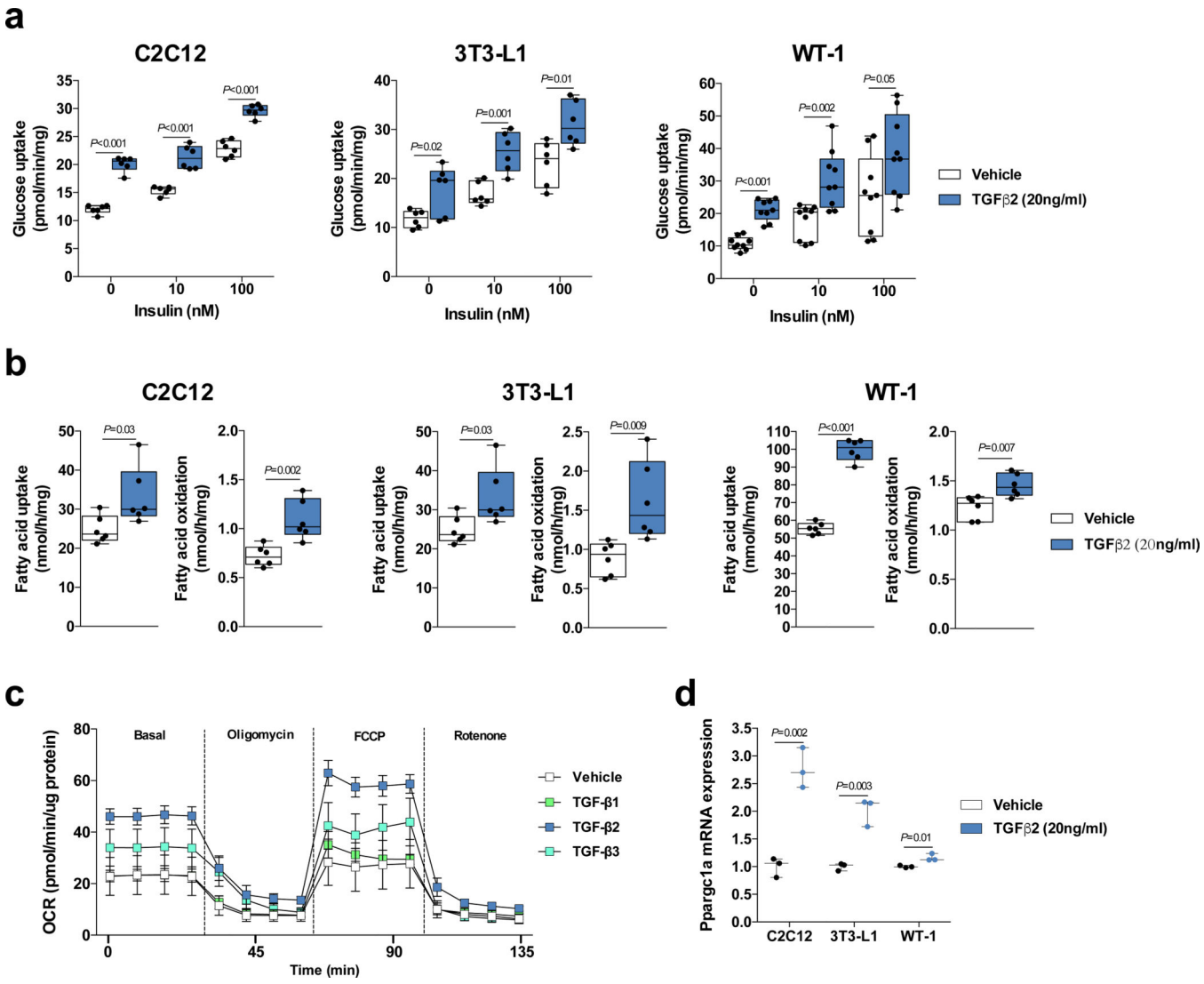

Figure 2.

Recombinant TGF-β2 treatment stimulates glucose uptake and oxygen consumption rate (OCR) *in vitro*. (**a**) Glucose uptake in C2C12 myotubes, 3T3-L1 adipocytes, and WT-1 brown adipocytes treated with TGF-β2; *n*=6 biological replicates for C2C12 myotubes and 3T3-L1 adipocytes. *n*=9 biological replicates for WT-1 brown adipocytes. (**b**) [^{14}C] palmitic acid uptake and oxidation in C2C12 myotubes, 3T3-L1 adipocytes and WT-1 brown adipocytes treated with TGF-β2; *n* = 6 biological replicates. (**c**) Extracellular flux analysis in C2C12 myotubes treated with TGF-β1, TGF-β2, or TGF-β3. *n*=4–6 technical-replicates wells. (**d**) Ppargc1a mRNA expression in C2C12 myotubes, 3T3-L1 adipocytes, and WT-1 brown adipocytes treated with TGF-β2; *n*=3 biological replicates. Data are presented as box plots (min, max, median, and 25th and 75th percentiles) with dots as individual values (**a**, **b** and **c**), or mean ± s.e.m (**c**). Unpaired two-tailed Student's t-test was used for **a, b** and **d**.

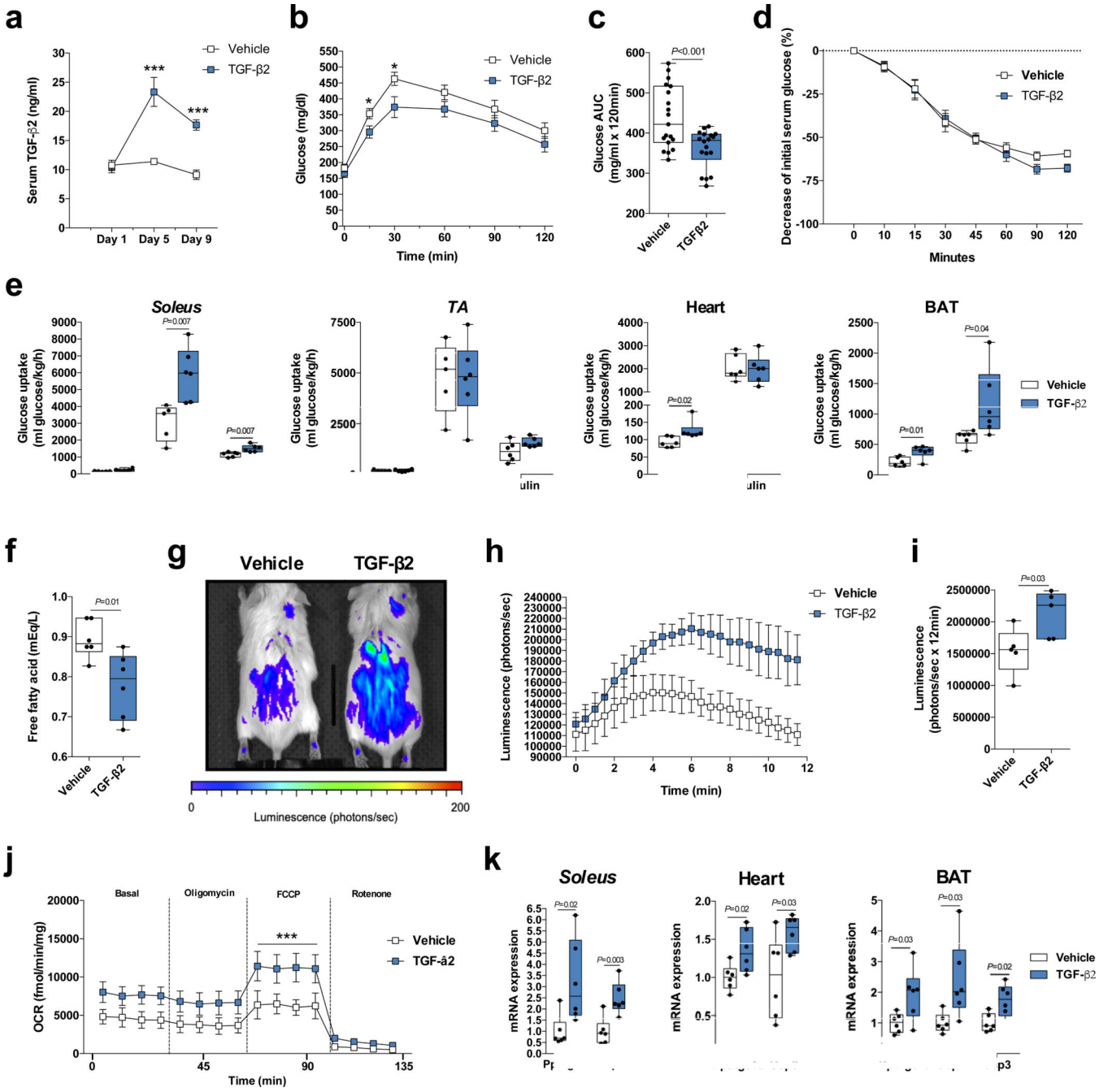

Figure 3.

TGF-β2 infusion via osmotic pump stimulates tissue glucose uptake and muscle oxygen consumption rate (OCR) in mice. (**a**) TGF-β2 serum concentration during TGF-β2 infusion; *n*=7 mice. (**b**) Glucose tolerance test (GTT) and (**c**) GTT area under the curve after nine days of TGF-β2 infusion; *n*=19 mice. (**d**) Insulin tolerance test (ITT); *n*=19 mice. (**e**) [^{3}H]-2-deoxyglucose uptake in *soleus*, *tibialis anterior* (*TA*), heart and BAT; *n*=5 or 6 mice. (**f**) Serum free fatty acid concentrations in mice; *n*=6 mice. (**g**) Representative image of luciferin-conjugated fatty acid uptake, (**h**) quantification of luciferin activity and (**i**) area

under the curve (AUC) in mice. n=5 mice. (**j**) OCR in *soleus* fibers; n=5 mice. (**k**) Ppargc1a, Ucp1, and Ucp3 mRNA relative expression in *soleus*, heart, and BAT; n=6 mice. Data are presented as box plots (min, max, median, and 25th and 75th percentiles) with dots as individual values (**c**, **e**, **f**, **i** and **k**), or mean ± s.e.m (**a**, **b**, **d**, **h** and **j)**. Unpaired two-tailed Student's t-test was used for **c**, **e**, **f**, **i** and **k**. ANOVA was used for **a**, **b**, **c**, **h** and **j**. When ANOVA showed P<0.05, Tukey's multiple comparisons tests were used with *P<0.05; ***P<0.001.

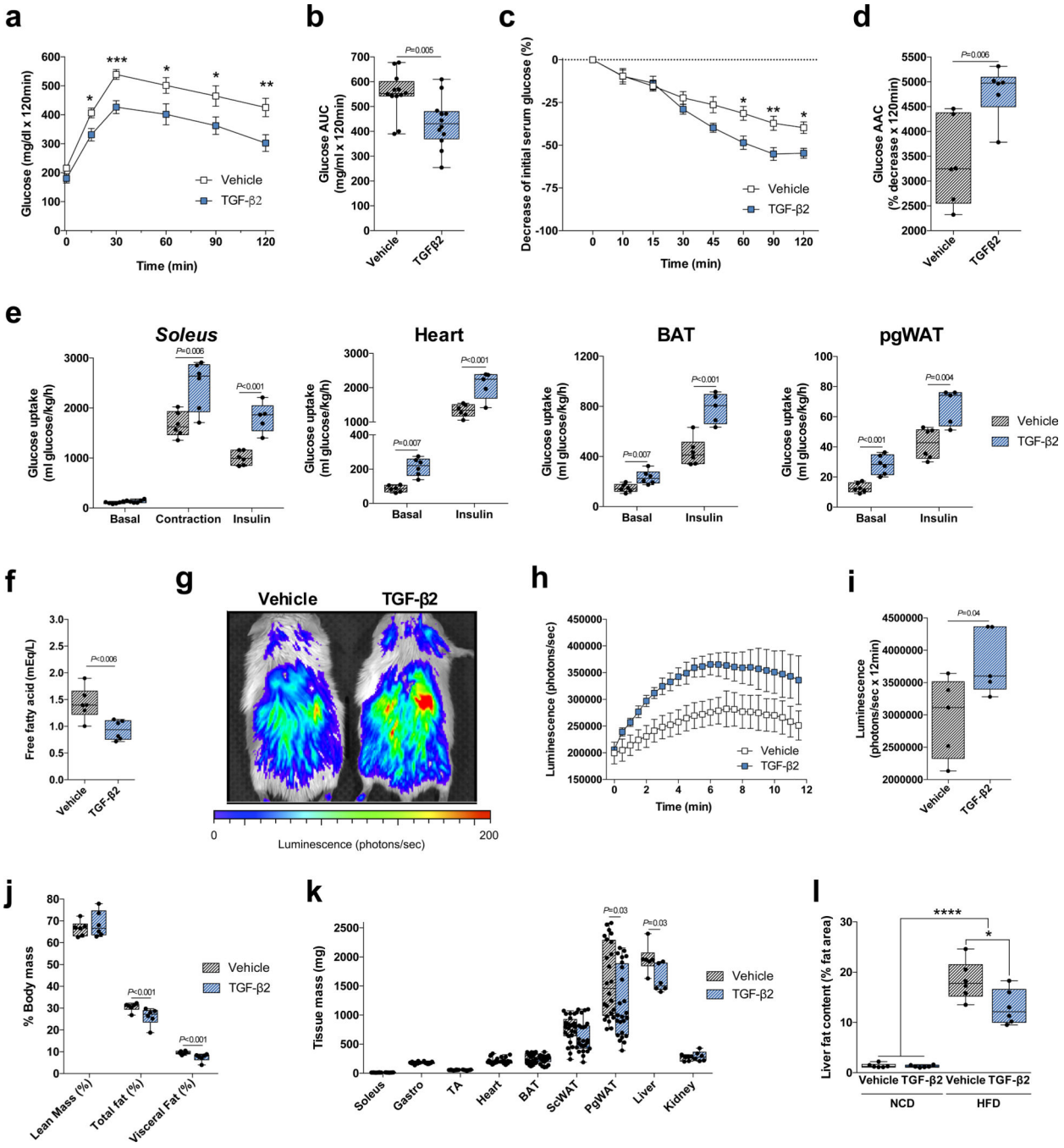

Figure 4.

TGF-β2 infusion via osmotic pump ameliorates the effects of a high fat diet in mice. (**a**) Glucose tolerance test (GTT) and (**b**) GTT area under the curve in high fat diet-fed (HFD) mice treated with TGF-β2; n=12 mice. (**c**) Insulin tolerance test (ITT) and (**d**) ITT area above the curve; n=6 mice. (**e**) [^{3}H]-2-deoxyglucose uptake in *soleus*, heart, BAT, and pgWAT; n=5 or 6 mice. (**f**) Serum free fatty acid concentrations in HFD mice; n=6 mice. (**g**) Representative image of luciferin-conjugated fatty acid uptake, (**h**) quantification of luciferin activity and (**i**) area under the curve (AUC) in mice. n=5 mice. (**j**) Lean, total fat and visceral

fat mass; n=6 mice. (**k**) Tissue mass; n=24 mice. (**l**) Liver fat content in normal chow diet-fed (NCD) or HFD mice; n=8 mice. Data are presented as box plots (min, max, median, and 25th and 75th percentiles) with dots as individual values (**b**, **d**, **e**, **f**, **i**, **j**, **k** and **l**), or mean ± s.e.m (**a**, **c**, and **h)**. Unpaired two-tailed Student's t-test was used for **b**, **d**, **e**, **f, i, j** and **k**. ANOVA was used for **a**, **c**, and **l**. When ANOVA showed P<0.05, Tukey's multiple comparisons tests were used with *P<0.05; **P<0.01, ***P<0.001, ****P<0.0001.

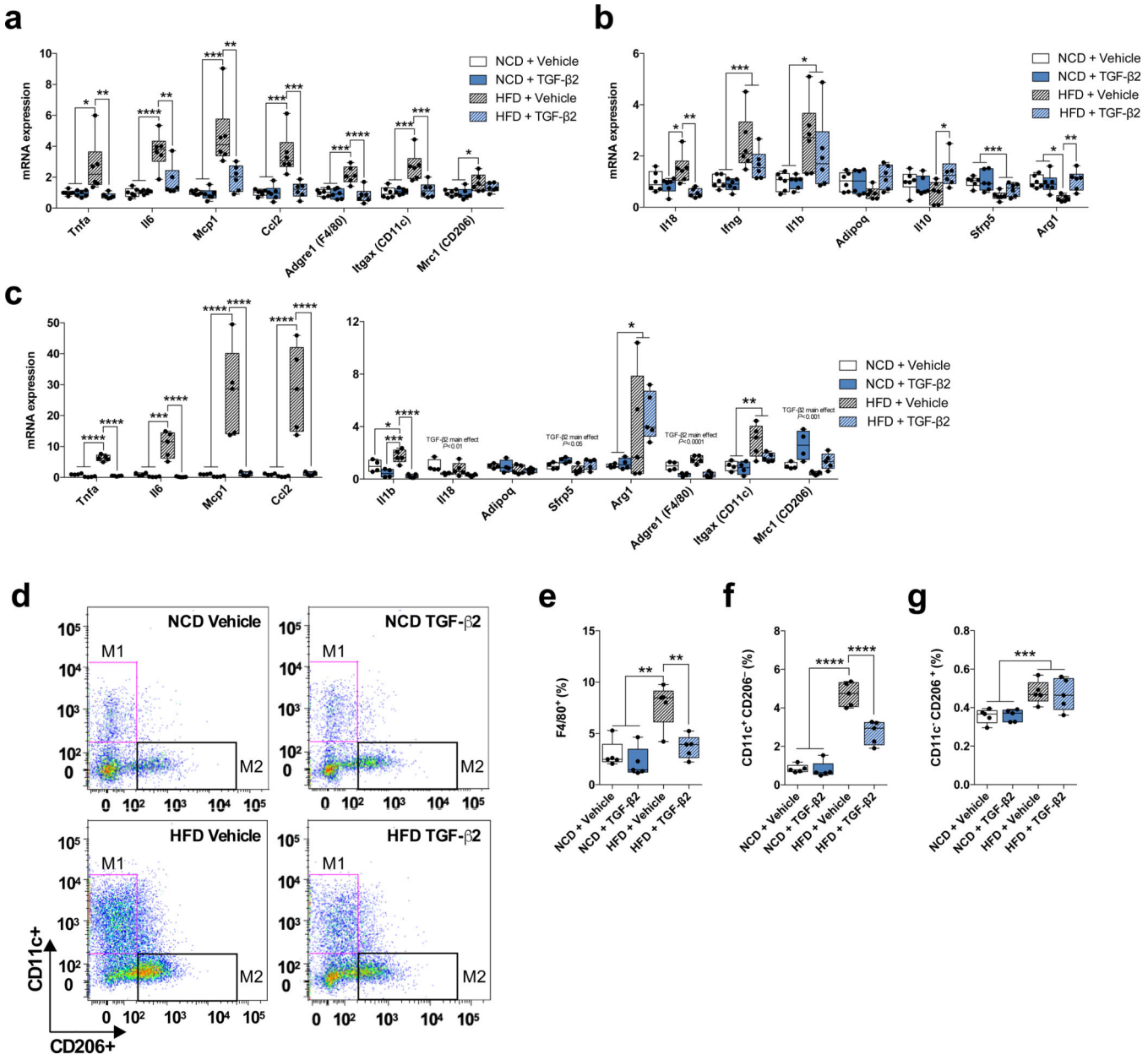

Figure 5.

TGF-β2 treatment attenuates high fat diet-induced inflammation in adipose tissue. (**a,b**) Expression of (**a**) pro-inflammatory and (**b**) anti-inflammatory markers in pgWAT in normal chow diet-fed (NCD) and HFD mice treated with TGF-β2; *n*=6 mice. (**c**) Levels of mRNA for inflammatory markers in peritoneal macrophages isolated from NCD and HFD mice and treated with TGF-β2; *n*=4 mice. (**d**) Representative image of flow cytometry experiment. (**e**) Percentage of macrophages (F4/80$^+$) infiltrated in pgWAT in NCD and HFD mice treated with TGF-β2; *n*=5 mice. (**f**) Percentage of M1 and (**g**) M2 macrophages infiltrated in pgWAT in NCD and HFD mice treated with TGF-β2; *n*=5 mice. Data are presented as box plots (min, max, median, and 25th and 75th percentiles) with dots as individual values (**a**, **b**, **c**, **e**, **f**, and **g**). ANOVA was used for **a**, **b**, **c**, **e**, **f** and **g**. When ANOVA showed $P<0.05$,

Tukey's multiple comparisons tests were used with *P<0.05; **P<0.01, ***P<0.001, ****P<0.0001.

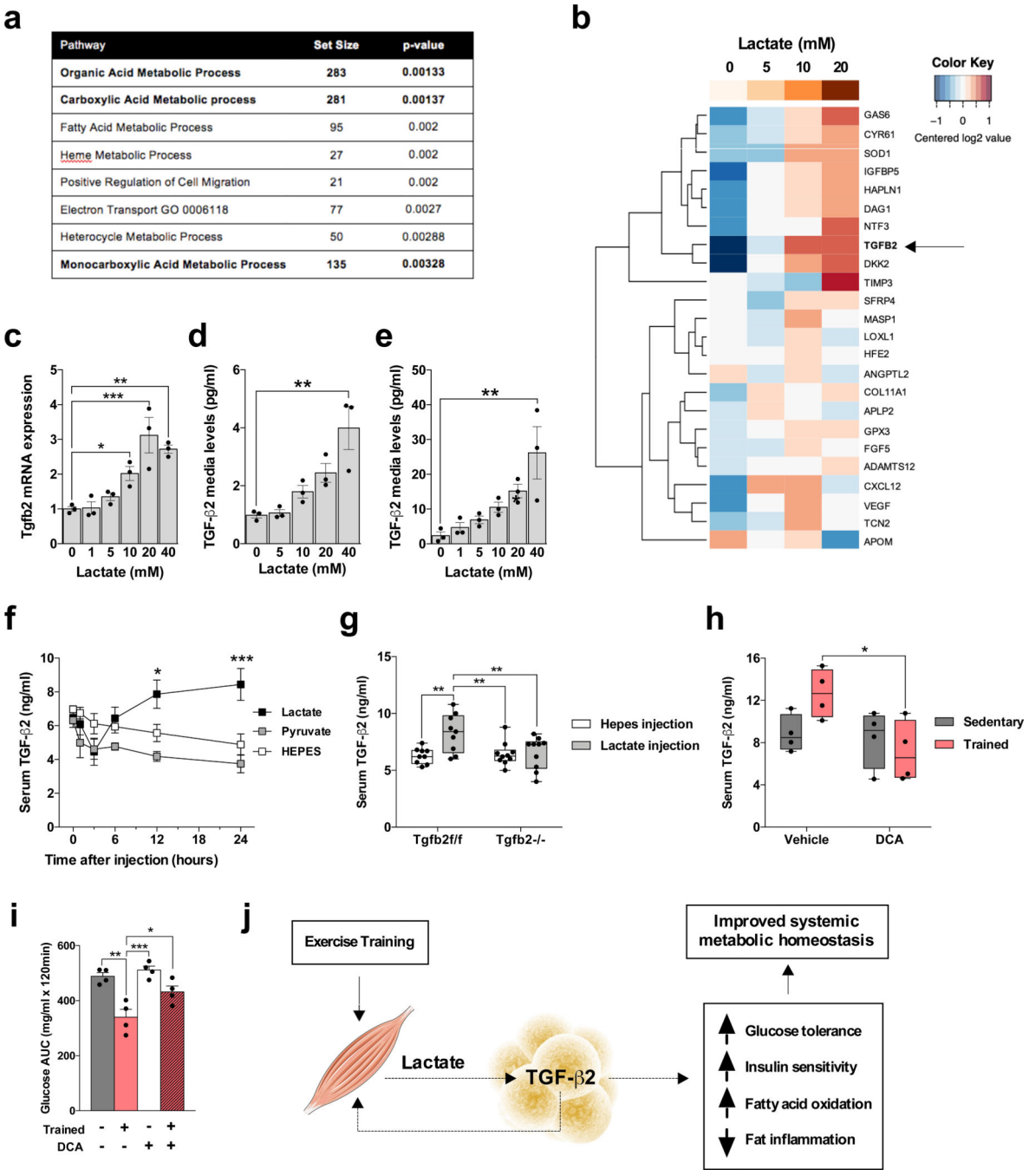

Figure 6.

Lactate produced by exercise training stimulates TGF-β2. (**a**) Most significant pathways correlated to Tgfb2 expression in scWAT microarray in trained mice. (**b**) Human adipocytes response to lactate. Putative adipokine genes selected from previous scWAT microarray of trained mice. -ΔCt data were centered for each row to have a mean of zero; a color bar representing lactate concentration is shown at the top. (**c**) Tgfb2 mRNA relative expression in human adipocytes treated with different concentrations of lactate; *n*=3 biological replicates. (**d,e**) TGF-β2 media concentration in (**d**) 3T3-L1 adipocytes and (**e**) human

adipocytes treated with lactate; n=3 biological replicates. (**f**) TGF-β2 serum concentration in mice injected with lactate, pyruvate, or vehicle (HEPES) intraperitoneally; n=4 mice. (**g**) Serum TGF-β2 concentration in $Tgfb2^{f/f}$ and $Tgfb2^{-/-}$ mice 24 hours after a lactate injection. (**h**) Serum TGF-β2 concentration in trained mice and/or daily treated with dichloroacetate (DCA) injections; n=4 mice. (**i**) Glucose tolerance test (GTT) area under the curve in trained mice after daily dichloroacetate (DCA) injections; n=4 mice. (**j**) Proposed model of exercise training effects on lactate-TGF-β2 signaling axis. Data are presented as box plots (min, max, median, and 25th and 75th percentiles) with dots as individual values (**g** and **h**), or mean ± s.e.m (**c**, **d**, **e**, **f**, and **i)**. ANOVA was used for **c**, **d**, **e**, **f**, **g**, **h** and **i**. When ANOVA showed P<0.05, Tukey's multiple comparisons tests were used with *P<0.05; **P<0.01, ***P<0.001.